modification of the dissipation rate equation is required to improve the response of the ASM to adverse pressure-gradient effects.

The second test case to be considered is the ONERA M6 wing at a Mach number $M_\infty = 0.8447$, an angle of attack $\alpha = 5.06$ deg, and a Reynolds number $Re = 11.7 \times 10^6$ based on the mean aerodynamic chord length.[16] A C–O grid used in this study has $193 \times 49 \times 33$ points in the streamwise, normal, and spanwise directions. The minimum normal spacing over the wing of 0.000015 $c_{\rm root}$ is used and a distance from the wing to the outer boundary of at least 7.95 $c_{\rm root}$ is considered. No wind-tunnel test corrections are employed for this case. Figure 3 shows a comparison of the computed surface pressure distributions with the experimental data at four different spanwise locations, $2y/B$. It is clear that the shock location and the surface pressure distributions predicted by the EASM are in good agreement with the experimental data and similar to the results reported[17] for the Johnson–King model, which has been highly tuned for airfoil flows. This is an encouraging result.

IV. Conclusion

A new EASM, which is derived from one of the most current second-order closures, has been applied to two aerodynamic test cases—one of which involves separation. The results clearly demonstrate the potential of the new model. Such EASMs have shown some improvement over the standard two-equation models because of their ability to accurately account for mild nonequilibrium effects and to give a realistic representation of the anisotropy of turbulence. However, this improvement still is limited by the dissipation rate equation, which fails to respond properly to adverse pressure gradients. A major research effort to correct this deficiency is currently underway.

Acknowledgments

The first and second authors would like to thank NASA Langley Research Center for support under Contracts NAS1-20059 and NAS1-19831. The fourth author acknowledges the support of the Office of Naval Research under Grant N00014-94-1-0088 (L. P. Purtell, Program Officer).

References

[1]Speziale, C. G., "Analytical Methods for the Development of Reynolds Stress Closures in Turbulence," *Annual Review of Fluid Mechanics*, Vol. 23, 1991, pp. 107–157.

[2]Wilcox, D. C., *Turbulence Modeling for CFD*, DCW Industries, Inc., La Cañada, CA, 1993.

[3]Launder, B. E., and Spalding, D. B., "The Numerical Computation of Turbulent Flows," *Computer Methods in Applied Mechanics and Engineering*, Vol. 3, 1974, pp. 269–289.

[4]Speziale, C. G., "On Nonlinear K–l and K–ε Models of Turbulence," *Journal of Fluid Mechanics*, Vol. 178, 1987, pp. 459–475.

[5]Rubinstein, R., and Barton, J. M., "Nonlinear Reynolds Stress Models and the Renormalization Group," *Physics of Fluids*, Vol. A2, No. 8, 1990, pp. 1472–1476.

[6]Pope, S. B., "A More General Effective Viscosity Hypothesis," *Journal of Fluid Mechanics*, Vol. 72, 1975, pp. 331–340.

[7]Gatski, T. B., and Speziale, C. G., "On Explicit Algebraic Stress Models for Complex Turbulent Flows," *Journal of Fluid Mechanics*, Vol. 254, 1993, pp. 59–78.

[8]Rodi, W., "A New Algebraic Relation for Calculating the Reynolds Stresses," *Zeitschrift für Angewandte Mathematik und Mechanik*, Vol. 56, 1976, pp. T219–T221.

[9]Abid, R., Rumsey, C., and Gatski, T. B., "Prediction of Non-Equilibrium Turbulent Flows with Explicit Algebraic Stress Models," *AIAA Journal*, Vol. 33, No. 11, 1995, pp. 2026–2031.

[10]Launder, B. E., Reece, G. J., and Rodi, W., "Progress in the Development of a Reynolds Stress Turbulence Closure," *Journal of Fluid Mechanics*, Vol. 68, 1975, pp. 537–566.

[11]Speziale, C. G., Sarkar, S., and Gatski, T. B., "Modeling the Pressure-Strain Correlation of Turbulence: An Invariant Dynamical Systems Approach," *Journal of Fluid Mechanics*, Vol. 227, 1991, pp. 245–272.

[12]Morrison, J. H., "A Compressible Navier–Stokes Solver with Two-Equation and Reynolds Stress Turbulence Closure Models," NASA CR4440, May 1992.

[13]Hinze, J. O., *Turbulence*, McGraw–Hill, New York, 1975.

[14]Launder, B., and Ying, Y., "Prediction of Flow and Heat Transfer in Ducts of Square Cross Section," *Proceedings of Institute of Mechanical Engineers*, Vol. 187, 1973, pp. 455–461.

[15]Cooke, P., McDonald, M., and Firmin, M., "Airfoil RAE2822—Pressure Distributions and Boundary Layer Wake Measurements," AGARD AR-138, May 1979.

[16]Schmitt, V., and Charpin, F., "Pressure Distribution on the ONERA M6 Wing at Transonic Mach Numbers," AGARD-AR-138, May 1979.

[17]Rumsey, C., and Vatsa, V. N., "Comparison of the Predictive Capabilities of Several Turbulence Models," *Journal of Aircraft*, Vol. 32, No. 3, 1995, pp. 510–514.

Development of a Rayleigh Scattering Measurement System for Hypersonic Wind-Tunnel Applications

Charles Tyler*
U.S. Air Force Wright Laboratory,
Wright–Patterson Air Force Base, Ohio 45433-7005

Introduction

RAYLEIGH scattering is a nonintrusive measurement technique, which has been used successfully over the last several years for simple reacting flows,[1] combustors,[2] and subsonic freejets.[3] Recently the Rayleigh scattering technique has been extended into the supersonic regime with limited quantitative results. Condensation and cluster formation have been found to have an adverse effect on Rayleigh scatter measurements.[4] Various efforts in eliminating such adverse effects and other unwanted biases, e.g., extraneous scattering off tunnel surfaces, have been made.

Although the construction of baffles for the elimination of stray laser beams has been found by others to reduce background scatter, such constructs do not eliminate laser glare off a model surface completely. Recently, a dual-line Rayleigh scatter system, using the green and yellow lines of a copper-vapor laser, has been developed and tested by Otugen et al.[5] This particular technique identifies and eliminates surface scatter background noise. Other recent techniques, which measure velocity, temperature, and density in supersonic and other high-speed flows, include filtered Rayleigh scattering and Raman excitation and lased-induced fluorescence imaging.[7] Filtered Rayleigh scattering is an alternate way of eliminating background scattering. These techniques solve the problem of surface scatter background noise; however, they do not address the problems associated with flow condensation.

In the past, a substantial amount of research regarding condensation in supercooled hypersonic flow has been performed.[8,9] Recently, Shirinzadeh et al.[10] performed experiments in a 15-in. Mach 6 high-temperature facility with the results that, in the absence of condensation, it is possible to obtain quantitative measurements of density using Rayleigh scattering techniques.

Experiments performed in a Mach 6 high Reynolds number facility were at a lower stagnation temperature of 556 K and higher stagnation pressures of 2.01 and 4.83 MPa. Density profiles, for a select location on a 8-deg half-angle blunt nose cone, obtained by Rayleigh scatter measurements were compared to computational fluid dynamics (CFD) results.

Equipment/Facility Discussion

The Rayleigh scatter measurement system was located at the Mach 6 high Reynolds number facility; an equipment schematic is shown in Fig. 1. A frequency-doubled Nd:YAG pulsed laser pumps two oscillator-amplifier, tunable dye lasers. The output from one

Received April 13, 1996; revision received July 11, 1996; accepted for publication Aug. 29, 1996; also published in *AIAA Journal on Disc*, Volume 2, Number 1. This paper is declared a work of the U.S. Government and is not subject to copyright protection in the United States.

*Aerospace Engineer, Wright Laboratory/Flight Dynamics Directorate/Aeromechanics Division. Member AIAA.

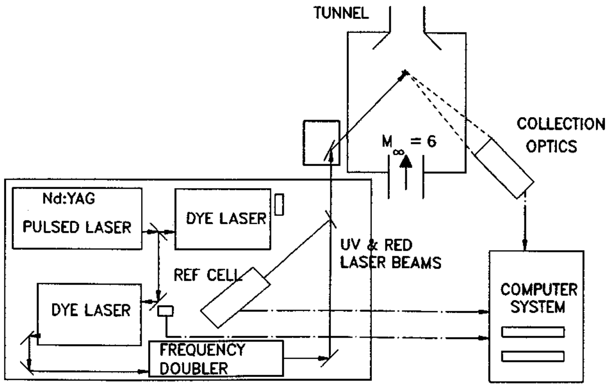

Fig. 1 Schematic of the Rayleigh scattering measurement system.

dye laser is blocked. The unblocked dye laser is tuned such that the wavelength of the exit beam is 613 nm. This exit beam is then frequency doubled using a beta-barium-borate doubling crystal resulting in a beam with a wavelength of 306.5 nm. As a result of the doubling process and optical configuration, the red beam, 613 nm, and the uv beam, 306.5 nm, are collinear.

The beam passes through a gas reference cell containing air at a known pressure and temperature. The reference cell provides a means of eliminating pulse-to-pulse laser power fluctuations. Two photomultiplier tubes (PMT) are mounted within the reference cell. The PMTs collect red and uv scattered light, respectively, and convert the light into signals, referred to as the reference signals. The reference signal is used to normalize the sample signal in the facility test section.

The beams passing through the reference cell are directed into the test section through a fused-silica window. Two 90-deg turning prisms steer the beam such that it enters the window on one side of the test section and strikes the wall on the other side. The scattered light from within the test cell is collected by a light collection system consisting of a 30-cm focal length planoconvex lens, bandpass filter and two PMTs. The angle of observation is perpendicular to the direction of incident light. The reference and sample signals are processed by a data acquisition computer system, which consists of gated integrators, an A/D converter, and a 286 IBM-compatible computer.

The Mach 6 high Reynolds number facility at Wright Laboratory is a blowdown tunnel, which uses dried, compressed air. The air is heated to 500–611 K by a heater bed of stainless steel balls prior to entering the stagnation chamber. The tunnel has an axisymmetric, 31.36-cm-diam nozzle contoured to produce an uniform flow, which has a calibrated center Mach number of 5.76 (Ref. 11). The tunnel was operated over a range of stagnation pressures, 0.69–6.9 MPa in increments of 0.69 MPa, at fixed stagnation temperatures, 511, 556, and 611 K. For stagnation pressures less than 4.1 MPa, the air exhausted from the tunnel is directed into a 2831 m^3 vacuum sphere; otherwise, the tunnel is exhausted to atmosphere.

Results

The main assumption of the Rayleigh scatter measurement system at U.S. Air Force Wright Laboratory is that Rayleigh coefficients are proportional to air density. In other words, there is a linear relationship between the air density and the intensity of the scattered light. With this understanding, initial tests were performed in the laboratory. As part of a calibration process intensity measurements were taken at an atmospheric and a very low-pressure condition; pressures and temperatures were obtained from static probes within the test section. Now, because intensities at two known density conditions were obtained, a line can be drawn that shows the relation between density and intensity. By using this relation, the surface scatter background noise can be determined and eliminated, where the slope is

$$M = \frac{I_2 - I_1}{\rho_2 - \rho_1} \tag{1}$$

and surface scatter is

$$b = I_1 - M \times \rho_1 \tag{2}$$

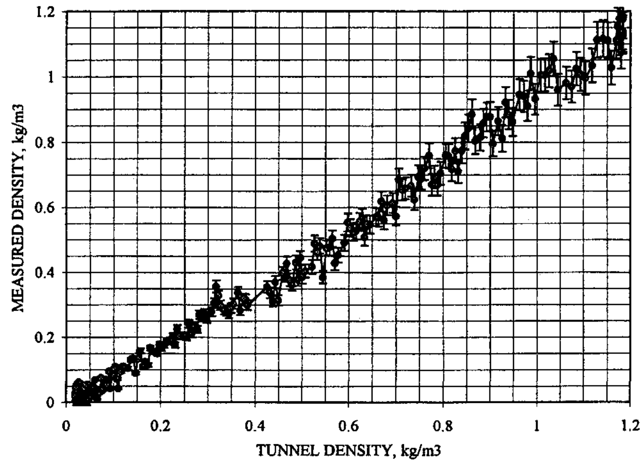

Fig. 2 Rayleigh scattering measurement system tracking of tunnel density.

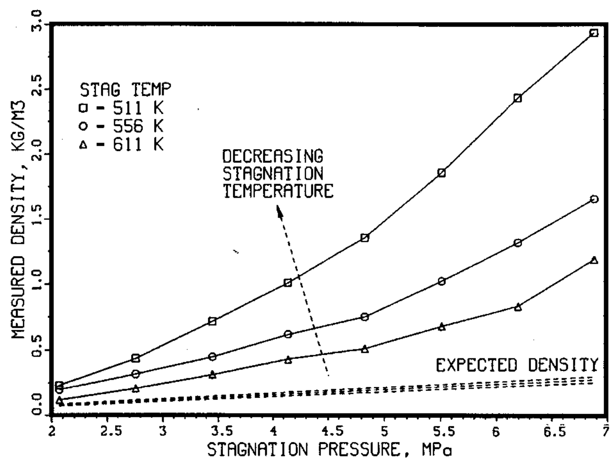

Fig. 3 Rayleigh scattering measurements for various tunnel conditions.

Once the calibration was completed the test section was slowly pumped down to a very low pressure. Rayleigh scatter measurements were performed during the evacuation process, tracking the density of the air in the test section to its lower limit of 0.019 kg/m^3, the error in the calculated densities is less than 10%. Figure 2 illustrates these tracking measurements.

Although large particles are absent from the flow during tunnel operation, higher than expected intensity signals were acquired when the tunnel was operating at the aforementioned hypersonic conditions. As shown in Fig. 3, the intensity of the signals diverges from the expected measurements quite dramatically for the lower stagnation temperatures. Even at the lowest stagnation temperature, 511 K, and the highest stagnation pressure, 6.9 MPa, condensation of the principle components of air, nitrogen, and oxygen should not occur; however, carbon dioxide, which exists in air as a minor component, condenses well before the saturation of nitrogen or oxygen. The condensation of carbon dioxide does not seriously affect the stream properties because of the small percentage in which it exists. However, a large number of nuclei are formed in the condensation of carbon dioxide, which then may act as nuclei for oxygen and nitrogen condensation. Even if the condensed carbon dioxide does not cause the primary constituents of air to condense, the carbon dioxide condensation particles formed still foul Rayleigh scatter measurements.

Under the belief that the condensation particles formed by the rapid expansion of the gas from the stagnation chamber are small and may possibly sublimate traveling through a strong shockwave,[12] measurements were made on a 8-deg half-angle blunt nose cone installed in the Mach 6 facility. Measurements were taken on a line perpendicular to the surface of the cone at a location of 12.7 cm back from the tip of the nose. Figure 4 shows the comparison between

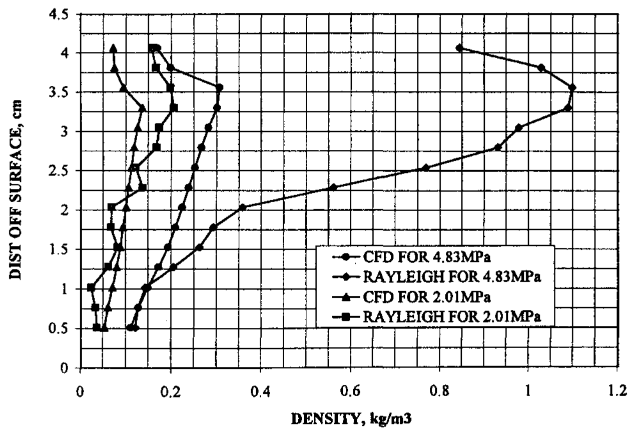

Fig. 4 Comparison of Rayleigh scattering measurements and CFD results.

Rayleigh scatter measurements and CFD results. Close to the surface of the cone the measurements agree quite well, while farther off the surface behind the shock wave and into the freestream it is apparent that the Rayleigh scatter measurements are substantially higher than expected. Although the quantitative results disagree, it is reassuring to see that qualitatively the two techniques, Rayleigh scattering and CFD, appear similar.

Conclusions

Extraneous surface scatter and scatter off condensation particles create difficulties in using Rayleigh scattering as a measurement technique in hypersonic flows. Fortunately, the surface scatter background noise can be eliminated by taking scattered intensity, readings at two known density conditions, obtaining the linear relation between density and scattered intensity, and calculating the level of extraneous surface scatter. Further work will be performed toward reduction and possible elimination of condensation effects hindering Rayleigh scattering measurement efforts.

Acknowledgments

The author thanks all of the people involved with the Rayleigh scattering instrumentation development test. The author appreciates the effort of work generated by the Mach 6 facility crew, as well as the pump house crew. The author would also like to thank the members of the Experimental Diagnostics section for all their patience, constant support, and helpful suggestions.

References

[1]Bill, R. G., Namer, I., Talbot, L., and Robben, F., "Density Fluctuations of Flame Grid Induced Turbulence," *Combustion and Flame*, Vol. 44, Nos. 1–3, 1982, pp. 277–285.

[2]Namazian, M., Talbot, L., Robben, F., and Cheng, R. K., "Two-Point Rayleigh Scattering Measurements in a V-Shaped Turbulent Flame," *19th Symposium on Combustion*, Combustion Inst., Pittsburgh, PA, 1982, pp. 487–493.

[3]Escoda, C., and Long, M. B., "Rayleigh Scattering Measurements of Gas Concentration Field in Turbulent Jets," *AIAA Journal*, Vol. 21, No. 1, 1983, pp. 81–84.

[4]Shirinzadeh, B., Hillard, M. E., and Exton, R. J., "Condensation Effects on Rayleigh Scattering Measurements in a Supersonic Wind Tunnel," *AIAA Journal*, Vol. 29, No. 2, 1991, pp. 242–246.

[5]Otugen, M. V., Seasholtz, R. J., and Annen, K. D., "Development of a Rayleigh Scattering System for Temperature Measurements," 4th International Conf. on Laser Anemometry Advancements and Applications, Fluids Engineering Div., American Society of Mechanical Engineers, Cleveland, OH, Aug. 1991.

[6]Miles, R. B., Lempert, W. R., and Forkey, J., "Instantaneous Velocity Fields and Background Suppression by Filtered Rayleigh Scattering," AIAA Paper 91-0357, Jan. 1991.

[7]Miles, R., Lempert, W., Forkey, J., Zhang, B., and Zhou, D., "Filtered Rayleigh and RELIEF Imaging of Velocity, Temperature, and Density in Hypersonic Flows for the Study of Boundary Layers, Shock Structures, Mixing Phenomena, and the Acquisition of In-Flight Air Data," *New Trends in Instrumentation for Hypersonic Research*, NATO Advanced Research Workshop, ONERA, Le Fauga-Mausae, France, 1992, pp. 5G.1–5G.8.

[8]Durbin, E. J., "Optical Methods Involving Light Scattering for Measuring Size and Concentration of Condensation Particles in Supercooled Hypersonic Flow," NACA TN 2441, Aug. 1951.

[9]Daum, F. L., and Gyarmathy, G., "Air and Nitrogen Condensation in Hypersonic Nozzle Flow," Aerospace Research Labs., ARL 65-169, Wright–Patterson AFB, OH, March 1967.

[10]Shirinzadeh, B., Balla, R. J., and Hillard, M. E., "Quantitative Density Measurements in a Mach 6 Flow Field Using the Rayleigh Scattering Technique," *International Congress on Instrumentation in Aerospace Simulation Facilities* (Wright–Patterson AFB, OH), Inst. of Electrical and Electronics Engineers, New York, 1995, pp. 13.1–13.7 (IEEE Paper 95-CH3482-7).

[11]Fiore, A. W., and Law, C. H., "Aerodynamic Calibration of the Aerospace Research Laboratories M=6 High Reynolds Number Facility," Aerospace Research Labs., ARL TR 75-0028, Wright–Patterson AFB, OH, Feb. 1975.

[12]Strecker, J. J. F., and Roth, P., "Particle Breakup in Weak Shock Waves: Preliminary Observations," *Journal of Aerosol Science*, Vol. 23, Suppl. 1, 1992, pp. S63–S66.

Vibration and Stability of Simply Supported Elliptical Plates

M. K. Sundaresan,* G. Radhakrishnan,*
and B. Nageswara Rao*
Vikram Sarabhai Space Center,
Trivandrum 695 022, India

Introduction

ELLIPTICAL plates are widely used as cover plates for cutouts in structural components. The precise determination of frequencies and critical compressive loads of elliptical plates involves considerable difficulties in the integration of the fourth-order partial differential equation. The fundamental frequency parameters of elliptical plates with clamped and simply supported end conditions are obtained by using different techniques.[1,2] The elastic stability of a circular plate under compressive force N uniformly distributed around the edge of the plate has been extensively investigated.[3] For the case of simply supported circular plates, the critical load parameter $\lambda_b (\equiv Na^2/D)$ is given by[3]

$$\lambda_b = \beta^2 \tag{1}$$

where β is the smallest root of the characteristic equation,

$$\beta J_0(\beta) - (1 - \nu) J_1(\beta) = 0$$

and where a is the radius of the circular plate, D is the flexural rigidity, J_0 and J_1 are zeroth- and first-order Bessel's functions, respectively, and ν is the Poisson's ratio. Reference 4 provides the details on the stability of a clamped elliptical plate, which was investigated in 1937 by Woinowsky-Krieger using the energy method. An approximate calculation for the stability of simply supported elliptical plates was also suggested based on the results for circular plates. Clamping the edges increases the critical stress by a factor of 3.5 in circular plates and by a factor of 4.0 in rectangular plates.

For an elliptical plate the factor should lie between 3.5 and 4, depending on the eccentricity of the ellipse. Hence, the values of the critical stress for a clamped elliptical plate should be divided by a factor of between 3.5 and 4 to obtain the critical stress for a simply supported elliptical plate. This criterion may yield the lower and upper bound solutions for the stability of simply supported elliptical plates.

Received Oct. 14, 1995; revision received July 25, 1996; accepted for publication July 26, 1996; also published in *AIAA Journal on Disc*, Volume 2, Number 1.

*Scientist/Engineer, Structural Engineering Group.